

An Unsymmetrical 5,15-Disubstituted Tetrabenzoporphyrin: Effect of Molecular Symmetry on the Packing Structure and Charge Transporting Property

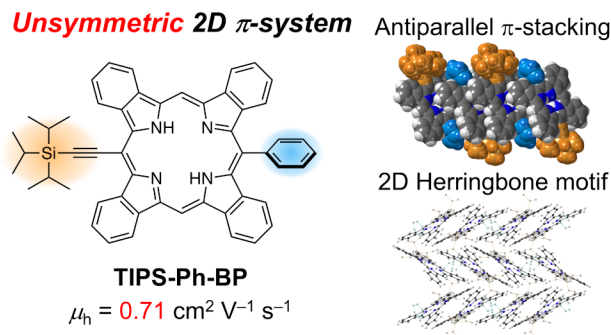
Kazuya Miyazaki, Kyohei Matsuo,* Hironobu Hayashi, Mitsuaki Yamauchi, Naoki Aratani, Hiroko Yamada*

Division of Materials Science, Graduate School of Science and Technology, Nara Institute of Science and Technology, 8916-5 Takayama-cho, Ikoma, Nara 630-0192, Japan

Institute for Chemical Research, Kyoto University, Gokasho, Uji, Kyoto 611-0011, Japan

Center for Basic Research on Materials, National Institute for Materials Science (NIMS), Sengen, Tsukuba, Ibaraki 305-0047, Japan

Supporting Information Placeholder



ABSTRACT: Molecular design strategy to control the crystal structure of two-dimensionally (2D) π -extended organic semiconductor has not been intensively explored. We synthesized an unsymmetric tetrabenzoporphyrin derivative (TIPS-Ph-BP) to demonstrate the effect of molecular symmetry on the crystal packing. TIPS-Ph-BP formed an antiparallel slipped π -stacking and 2D herringbone-like structure. Unsymmetric structure would make 2D π -stacking more stable than one-dimensional columnar structure to counteract steric and electronic imbalance in the crystal. As a result, TIPS-Ph-BP achieved the high hole mobility of $0.71 \text{ cm}^2 \text{ V}^{-1} \text{ s}^{-1}$.

One of the key issues in the development of organic field-effect transistor (OFET) materials is the improvement of charge mobility. Since charge mobility depends on intermolecular interactions in solid state, it is important to control the crystal structure.^{1–4} In the current mainstream OFET materials such as acenes and heteroacenes, which have one-dimensionally (1D) extended polycyclic aromatic frameworks, the effect of substitution on the crystal structure has been intensively studied.^{5–9} For examples, alkyl chain substitutions typically provide layer-by-layer lamella structure, in which aromatic cores are arranged in a herringbone motif.^{10–13} On the other hand, some of bulky (trialkylsilyl)ethynyl substituted derivatives such as 6,13-bis(triisopropylsilyl)ethynyl pentacene (TIPS-pentacene) have been known to afford the brickwork packing.^{14–17} In comparison, two-dimensionally (2D) extended π -conjugated molecules tend to form a sandwich herringbone, a cofacial herringbone, and a 1D columnar structure due to their enhanced π - π interaction.^{18,19} In addition, little is known about a versatile molecular design that would give a crystal structure suitable for OFET application.^{20–22} The 2D π -systems are expected to improve the thermal

stability of the crystalline phase because molecular rotation in the crystal can be suppressed compared to linear acene analogues.^{23,24} Furthermore, it is possible to have optical absorption in the visible to near-infrared region, which has the potential to lead to the development of new functions, such as application to phototransistors.²⁵

Tetrabenzoporphyrin (BP) is a useful building block as an organic semiconductor due to its chemical stability, large absorption coefficient in visible region, and strong π -stacking interaction. We previously synthesized 5,15-bis(triisopropylsilyl)ethynyl tetrabenzoporphyrin (TIPS-BP), its metal complexes, and diazaporphyrin analogue (Figure 1a).^{26–29} Free-base TIPS-BP shows unique polymorphism with different π -stacking manners.³⁰ One polymorph consists of 1D columnar π -stacking motif and exhibited moderate maximum hole mobility of $0.027 \text{ cm}^2 \text{ V}^{-1} \text{ s}^{-1}$ for thin-film OFETs. In another polymorph, TIPS-BP forms the brickwork packing structure as TIPS-pentacene and exhibited excellent OFET properties with a maximum hole mobility of $1.1 \text{ cm}^2 \text{ V}^{-1} \text{ s}^{-1}$. However, most of its metal complexes and diazaporphyrin analogue formed 1D columnar

structure. In addition, even in the case of thin films with brickwork structure, it was necessary to carefully optimize the deposition conditions. Hence, a rational molecular design for selective formation of 2D π -stacking of BP derivatives is desired.

In this study, we devised a method to control the crystal structure of 5,15-substituted BP derivatives by structural modification. 1D columnar packing and 2D brickwork packing of TIPS-BP consist of cross-stacking structure and slipped stacking structure, respectively (Figure S1). Because of the highly extended π -skeleton of BP, it is preferable to kinetically form cross-stack structure with large molecular overlap, thereby making the 1D columnar packing stable. If the substituents at 5- and 15-positions are different, i.e., unsymmetric derivatives, cross-stacking dimer is still kinetically favored, but the 1D columnar structure grown from it would lose central and translational symmetry. Thus, its aggregated crystal structure would be thermodynamically unfavorable because the steric and electrostatic imbalance could not be completely canceled (Figure 1b). On the other hand, if the molecules form slipped π -stacking in an antiparallel orientation, the steric and electrostatic imbalance could be counteract and the symmetry of the crystal structure would be maintained even for the unsymmetric molecule. Therefore, we expected that a 2D packing structure suitable for OFETs would become thermodynamically stable for the unsymmetric derivatives. Recently, it was reported that unsymmetric substitution on the heteroacenes with an alkyl chain enhances to form bilayer-type crystal structure.^{13,31,32} However, the effect of unsymmetric substitution on the crystal structure of 2D π -conjugated molecules has not been elucidated.

Herein, we designed and synthesized an unsymmetric BP derivative TIPS-Ph-BP, which has two substituents of different sizes at *meso* positions (Figure 1a). Its bulky triisopropylsilyl ethynyl (TIPS-ethynyl) group can enhance solubility, while the other compact phenyl group, in an orthogonal configuration perpendicular to the BP skeleton, would inhibit the formation of face-to-face π -stacking and instead form slipped stacking. As expected, TIPS-Ph-BP showed 2D packing in its crystal structure and the maximum hole mobility of the OFET prepared by drop-casting was $0.71 \text{ cm}^2 \text{ V}^{-1} \text{ s}^{-1}$, which is comparable to the hole mobility of TIPS-BP in 2D brickwork packing.

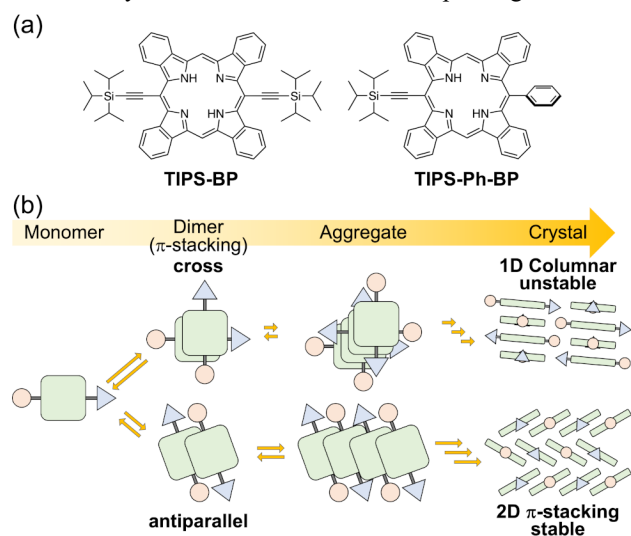
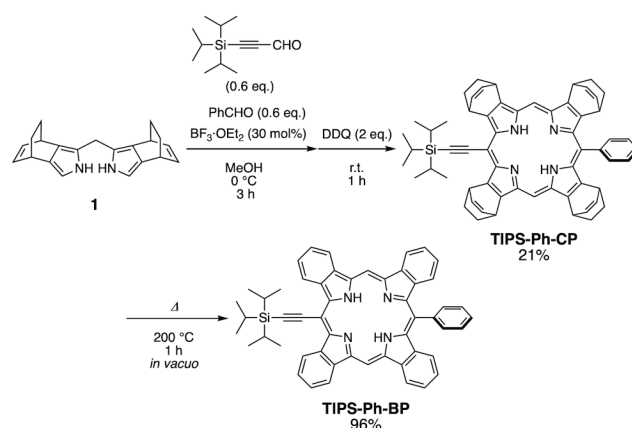


Figure 1. (a) Molecular structures of TIPS-BP and TIPS-Ph-BP. (b) Schematic representation of possible crystal structures for unsymmetric BP derivatives.

Scheme 1 shows the synthesis of TIPS-Ph-BP. Unsymmetric TIPS-Ph-CP was synthesized as precursor by [2+2] acid-catalyzed condensation reaction using two kinds of aldehydes.³³ Dipyrrromethane **1** was treated with 3-(triisopropylsilyl)propionaldehyde and benzaldehyde in the presence of borontrifluoride etherate, followed by oxidation with 2,3-dichloro-5,6-dicyano-1,4-benzoquinone (DDQ). Unsymmetric TIPS-Ph-CP was isolated by alumina column chromatography and recrystallization in 21% yield. This isolated yield is moderate compared to those of symmetric CP derivatives reported (7–57%^{24,26,33–35}). Even so, this could be attributed to the intrinsic problem that the yield of unsymmetric products is statistically up to 50%. Then, TIPS-Ph-CP was heated at 200 °C in a glass tube oven under vacuum to afford TIPS-Ph-BP in 96%. The high thermal stability of TIPS-Ph-TBP was confirmed by thermogravimetry–differential thermal analysis (TG-DTA) (Figure S2). The 5% weight loss temperature (T_{ds}) was 372 °C and no peaks were observed at temperatures below T_{ds} in the DTA curve.

Scheme 1. Synthesis of TIPS-Ph-BP.



To reveal the electronic differences due to the substituent, the UV-visible absorption and fluorescence spectra of TIPS-Ph-BP in chloroform were measured and compared with those of TIPS-BP²⁹ (Figure 2). As a result, both the Soret and Q bands in absorption spectrum of TIPS-Ph-BP blue-shifted. Similarly, the fluorescence wavelength blue-shifted from 716 nm to 690 nm. This would be due to the perpendicular configuration of the phenyl group with respect to BP skeleton, which results in contracted π conjugation than that of the ethynyl group. The absolute fluorescence quantum yield (Φ_{FL}) and fluorescence lifetime (τ) of TIPS-Ph-BP solution were 18% and 7.2 ns, respectively (Figure S3). According to these values, the radiative decay rate constant (k_r) and nonradiative decay rate constant (k_{nr}) were calculated to be $2.5 \times 10^7 \text{ s}^{-1}$ and $1.1 \times 10^8 \text{ s}^{-1}$, respectively. The almost equivalent k_r values for TIPS-Ph-BP and TIPS-BP ($2.1 \times 10^7 \text{ s}^{-1}$) correspond with their comparable molar absorption coefficient (ϵ) at first Q-band, while the smaller k_{nr} values for TIPS-Ph-BP than that of TIPS-BP ($1.9 \times 10^8 \text{ s}^{-1}$) can be attributed to the suppression of intramolecular rotation by introduction of perpendicular Ph group. The cyclic voltammetry (CV) also revealed substitution effect on the electrochemical property. TIPS-Ph-BP exhibited two reversible oxidation waves of $E_{\text{ox}} = 0.10$ and 0.31 V (vs. Fc/Fc^+) and a reversible reduction wave of $E_{\text{red}} = -1.61$ V (Figure S4). Compared to the redox potential of TIPS-BP, the first E_{ox} of TIPS-Ph-BP was positively shifted while its E_{red} was negatively shifted. This result suggests

that TIPS-Ph-BP has slightly larger HOMO–LUMO gap than TIPS-BP, similar to the blue-shift of its absorption wavelengths.

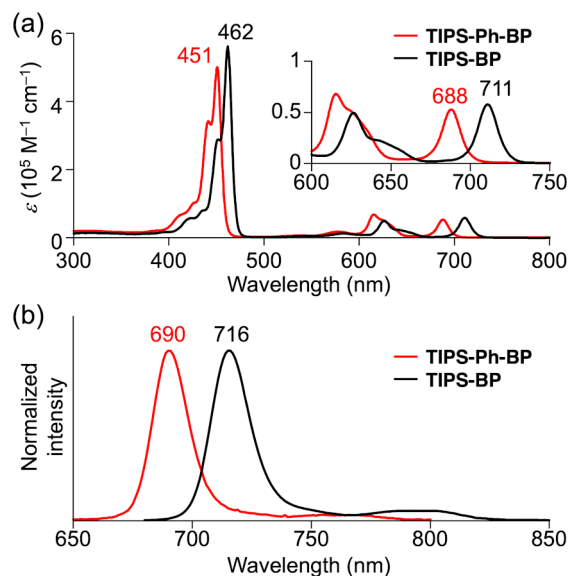


Figure 2. (a) UV-vis absorption and (b) fluorescence spectra of TIPS-Ph-BP and TIPS-BP in chloroform. ($\lambda_{\text{ex}} = 450 \text{ nm}$)

The single crystals of TIPS-Ph-BP suitable for X-ray diffraction measurement were prepared from chloroform and octane solution using a vapor diffusion method. The molecular structure and packing structure of TIPS-Ph-BP are shown in Figures 3 and S6–8. TIPS-Ph-BP had a bent TIPS-ethynyl group and a perpendicular Ph group. The dihedral angle between BP core and Ph group was 87.6° . Interestingly, BP core of TIPS-Ph-BP in the crystal was slightly contorted, unlike that of TIPS-BP which was highly planar. The dihedral angles between the two benzene rings across the free *meso* positions were 6.8° and 20.7° , respectively. In the crystal packing, TIPS-Ph-BP exhibited layered structure along the crystallographic *a*-axis (Figure S7). As expected, TIPS-Ph-BP formed a slipped π -stacking structure with an antiparallel manner in the layer (Figure 3a). Moreover, the BP cores are arranged in a herringbone-like motif (Figure 3b). A closer look at the π -stacking direction revealed two different stacking structures. In the pair A, the overlap of π -conjugated planes was large and the intermolecular distance between the BP centers was as close as 5.96 \AA , whereas in the pair B, only one isoindole ring overlapped each other and the intermolecular distance was calculated to be 7.96 \AA (Figure S8). Moreover, the interplane distance of 3.40 \AA for pair A was slightly closer than that of 3.43 \AA for pair B. These indicate that TIPS-Ph-BP has a local dimeric structure in the crystal like the sandwich herringbone structure. To discuss charge transport property in detail, the charge transfer integrals (t) of the HOMO between the neighboring molecular pairs were calculated using ADF program³⁶ (Figure S9 and Table S4). Along the π -stacking direction (the crystallographic *b*-axis), the t values for pairs A and B were very different and were calculated to be 62.3 and 15.9 meV , respectively. On the other hand, t values along the crystallographic *c*-axis were moderate and in the range of 3.1 – 10.7 meV . Although the packing structure of TIPS-Ph-BP is not an ideal 2D electronic structure because of the nonequivalent t values in each direction, TIPS-Ph-BP is expected to show good hole mobility because the t values are above a certain level in any direction.

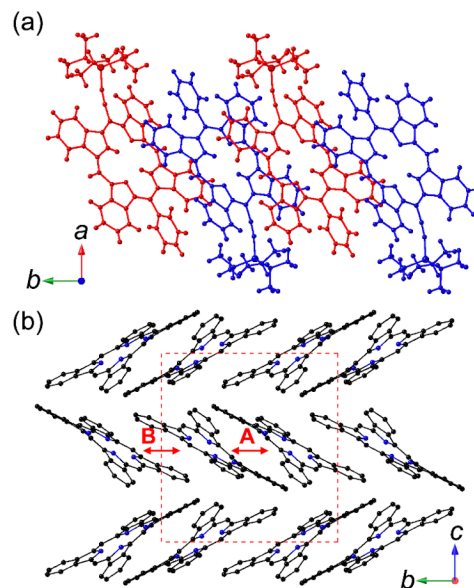


Figure 3. Crystal structures of TIPS-Ph-BP: (a) π -stacking structure viewed along *c*-axis; (b) Packing structure viewed along *a*-axis. Substituents and hydrogen atoms are omitted for clarity.

We fabricated the OFET devices using TIPS-Ph-BP. After examining various deposition conditions, plate-like crystals were obtained reproducibly by slow vapor diffusion of octane into a chlorobenzene solution of TIPS-Ph-BP on the substrate. Then, source and drain electrodes (gold, 30 nm) were vacuum deposited on the obtained crystals to afford top-contact bottom-gate FETs (Figures S10 and S11). The transfer and output characteristics are shown in Figures 4 and S12. The OFETs showed the best and average hole mobilities of 0.71 and $0.55 \text{ cm}^2 \text{ V}^{-1} \text{ s}^{-1}$, respectively. This maximum mobility is slightly lower than $2.16 \text{ cm}^2 \text{ V}^{-1} \text{ s}^{-1}$ of single crystal FET of free-base TIPS-BP, but higher than 0.12 and $0.16 \text{ cm}^2 \text{ V}^{-1} \text{ s}^{-1}$ of its zinc(II) and copper(II) complexes, respectively.²⁸ The out-of-plane X-ray diffraction measurement of the OFET device showed one diffraction peak at 4.5° , which should correspond to the (100) diffraction of single crystal structure (Figure S13). Furthermore, face index analysis of TIPS-Ph-BP based on the single crystal X-ray crystallography revealed that the crystal face with the largest area of the platelet crystal corresponds to the (100) face (Figure S5). These results suggest that the crystallographic *bc* plane, which contains π -stacking direction, is parallel to the substrate and current flow direction (Figure S14). Despite the herringbone-like packing, hole mobility of TIPS-Ph-BP was moderate. This is probably due to the local dimeric structure in the crystal packing similar to the results for single crystal FETs of TIPS-BP metal complexes, where the long-range charge transport was suppressed by triad-like structure in columnar π -stacking.²⁸

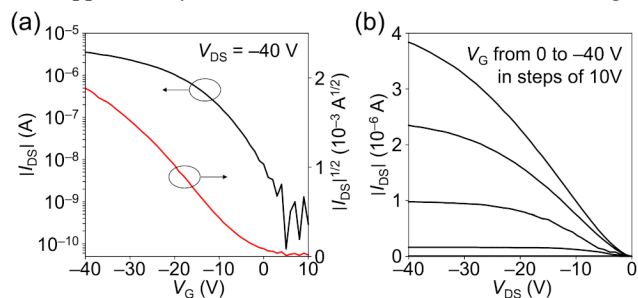


Figure 4. (a) Transfer and (b) output characteristics of the best-performing OFET using TIPS-Ph-BP.

In summary, we have synthesized an unsymmetric 5,15-disubstituted BP derivative to study the influence of molecular symmetry on the crystal structure of 2D extended π -conjugated systems. TIPS-Ph-BP formed a dimeric herringbone packing consisting of slipped π -stacking with an antiparallel manner in the crystal. OFETs using TIPS-Ph-BP achieved the maximum hole mobility of $0.71 \text{ cm}^2 \text{ V}^{-1} \text{ s}^{-1}$ due to the partially 2D packing structure. This strategy could be used to control the crystal structures of various 2D extended π -conjugated systems.

ASSOCIATED CONTENT

Data Availability Statement

The data underlying this study are available in the published article and its Supporting Information.

Supporting Information

The Supporting Information is available free of charge on the ACS Publications website.

Experimental details, NMR and HRMS data, TG-DTA data, X-ray crystallographic data, photophysical and electrochemical data, and OFET characteristics (PDF)

Accession Codes

CCDC 2286511 contains the supplementary crystallographic data for this paper. This data can be obtained free of charge via www.ccdc.cam.ac.uk/data_request/cif, or by emailing da-ta-request@ccdc.cam.ac.uk, or by contacting The Cambridge Crystallographic Data Centre, 12 Union Road, Cambridge CB2 1EZ, UK; fax: +44 1223 336033.

AUTHOR INFORMATION

Corresponding Author

Kyohei Matsuo – Institute for Chemical Research, Kyoto University, Gokasho, Uji, Kyoto 611-0011, Japan; orcid.org/0000-0002-2472-9459; E-mail: matsuo.kyohei.2x@kyoto-u.ac.jp

Hiroko Yamada – Institute for Chemical Research, Kyoto University, Gokasho, Uji, Kyoto 611-0011, Japan; orcid.org/0000-0002-2138-5902; E-mail: hyamada@sci.kyoto-u.ac.jp

Authors

Kazuya Miyazaki – Division of Materials Science, Graduate School of Science and Technology, Nara Institute of Science and Technology, 8916-5 Takayama-cho, Ikoma, Nara 630-0192, Japan
Hironobu Hayashi – Center for Basic Research on Materials, National Institute for Materials Science (NIMS), Sengen, Tsukuba, Ibaraki 305-0047, Japan; orcid.org/0000-0002-7872-3052

Mitsuaki Yamauchi – Institute for Chemical Research, Kyoto University, Gokasho, Uji, Kyoto 611-0011, Japan; orcid.org/0000-0003-0005-5960

Naoki Aratani – Division of Materials Science, Graduate School of Science and Technology, Nara Institute of Science and Technology, 8916-5 Takayama-cho, Ikoma, Nara 630-0192, Japan; orcid.org/0000-0002-3181-6526

Notes

The authors declare no competing financial interest.

ACKNOWLEDGMENT

This work was partly supported by the JSPS KAKENHI Grant No. JP22K05255 for KM, JP22K19067 and JP23H01787 for NA, JP20H05833 and JP20H00379 for HY and by ISHIZUE 2023 of

Kyoto University for HY. NMR measurements were supported by the Joint Usage/Research Center (JURC) at the Institute for Chemical Research, Kyoto University. We thank Ms. Akiko Fujihashi (Kyoto University) for HRMS measurements.

REFERENCES

- (1) Coropceanu, V.; Cornil, J.; da Silva Filho, D. A.; Olivier, Y.; Silbey, R.; Brédas, J.-L. Charge Transport in Organic Semiconductors. *Chem. Rev.* **2007**, *107*, 926–952.
- (2) Mas-Torrent, M.; Rovira, C. Role of Molecular Order and Solid-State Structure in Organic Field-Effect Transistors. *Chem. Rev.* **2011**, *111*, 4833–4856.
- (3) Takimiya K.; Shinamura, S.; Osaka, I.; Miyazaki, E. Thienoacene-Based Organic Semiconductors. *Adv. Mater.* **2011**, *23*, 4347–4370.
- (4) Wang, C.; Dong, H.; Hu, W.; Liu, Y.; Zhu, D. Semiconducting π -Conjugated Systems in Field-Effect Transistors: A Material Odyssey of Organic Electronics. *Chem. Rev.* **2012**, *112*, 2208–2267.
- (5) Anthony, J. E. Functionalized Acenes and Heteroacenes for Organic Electronics. *Chem. Rev.* **2006**, *106*, 5028–5048.
- (6) Yao, Z.-F.; Wang, J.-Y.; Pei, J. Control of π - π Stacking via Crystal Engineering in Organic Conjugated Small Molecule Crystals. *Cryst. Growth Des.* **2018**, *18*, 7–15.
- (7) Wang, C.; Nakamura, H.; Sugino, H.; Takimiya, K. Methylthioated Benzo[1,2-*b*:4,5-*b'*]dithiophenes: A Model Study to Control Packing Structures and Molecular Orientation in Thienoacene-Based Organic Semiconductors. *Chem. Commun.* **2017**, *53*, 9594–9597.
- (8) Wang, J.; Chu, M.; Fan, J.-X.; Lau, T.-K.; Ren, A.-M.; Lu, X.; Miao, Q. Crystal Engineering of Biphenylene-Containing Acenes for High-Mobility Organic Semiconductors. *J. Am. Chem. Soc.* **2019**, *141*, 3589–3596.
- (9) Mori, T.; Yasuda, T. U-Shaped Heteroacenes Embedded with Heavy Chalcogen Atoms: Unique Bilayer Self-Organization of Crooked π -Cores Enabling Efficient Charge Transport. *Adv. Electron. Mater.* **2021**, *7*, 2001052.
- (10) Izawa, T.; Miyazaki, E.; Takimiya, K. Molecular Ordering of High-Performance Soluble Molecular Semiconductors and Re-evaluation of Their Field-Effect Transistor Characteristics. *Adv. Mater.* **2008**, *20*, 3388–3392.
- (11) Yang, Y. S.; Yasuda, T.; Kakizoe, H.; Mieno, H.; Kino, H.; Tateyama, Y.; Adachi, C. High Performance Organic Field-Effect Transistors Based on Single-Crystal Microribbons and Microsheets of Solution-Processed Dithieno[3,2-*b*:2',3'-*d'*]thiophene Derivatives. *Chem. Commun.* **2013**, *49*, 6483–6485.
- (12) Okamoto, T.; Mitsui, C.; Yamagishi, M.; Nakahara, K.; Soeda, J.; Hirose, Y.; Miwa, K.; Sato, H.; Yamano, A.; Matsushita, T.; Uemura, T.; Takeya, J. V-Shaped Organic Semiconductors with Solution-Processability, High Mobility, and High Thermal Durability. *Adv. Mater.* **2013**, *25*, 6392–6397.
- (13) Minemawari, H.; Tanaka, M.; Tsuzuki, S.; Inoue, S.; Yamada, T.; Kumai, R.; Shimo, Y.; Hasegawa, T. Enhanced Layered-Herringbone Packing due to Long Alkyl Chain Substitution in Solution-Processable Organic Semiconductors. *Chem. Mater.* **2017**, *29*, 1245–1254.
- (14) Anthony, J. E.; Brooks, J. S.; Eaton, D. L.; Parkin, S. R. Functionalized Pentacene: Improved Electronic Properties from Control of Solid-State Order. *J. Am. Chem. Soc.* **2001**, *123*, 9482–9483.
- (15) Tang, M. L.; Reichardt, A. D.; Miyaki, N.; Stoltenberg, R. M.; Bao, Z. Ambipolar, High Performance, Acene-Based Organic Thin Film Transistors. *J. Am. Chem. Soc.* **2008**, *130*, 6064–6065.
- (16) Zeidell, A. M.; Jennings, L.; Frederickson, C. K.; Ai, Q.; Dressler, J. J.; Zakharov, L. N.; Risko, C.; Haley, M. M.; Jurchescu, O. D. Organic Semiconductors Derived from Dinaphtho-Fused *s*-Indacenes: How Molecular Structure and Film Morphology Influence Thin-Film Transistor Performance. *Chem. Mater.* **2019**, *31*, 6962–6970.
- (17) Jousselin-Oba, T.; Mamada, M.; Marrot, J.; Maignan, A.; Adachi, C.; Yassar, A.; Frigoli, M. Excellent Semiconductors Based on Tetracenotetracene and Pentacenopentacene: From Stable Closed-Shell to Singlet Open-Shell. *J. Am. Chem. Soc.* **2019**, *141*, 9373–9381.

- (18) Desiraju, G.R.; Gavezzotti, A. From Molecular to Crystal Structure; Polynuclear Aromatic Hydrocarbons. *J. Chem. Soc. Chem. Commun.* **1989**, 122, 621–623.
- (19) Yu, P.; Zhen, Y.; Dong, H.; Hu, W. Crystal Engineering of Organic Optoelectronic Materials. *Chem.* **2019**, 5, 2814–2853.
- (20) Dong, S.; Bao, C.; Tian, H.; Yan, D.; Geng, Y.; Wang, F. ABAB-Symmetric Tetraalkyl Titanyl Phthalocyanines for Solution Processed Organic Field-Effect Transistors with Mobility Approaching $1\text{ cm}^2\text{ V}^{-1}\text{ s}^{-1}$. *Adv. Mater.* **2013**, 25, 1165–1169.
- (21) Zhang, L.; Fonari, A.; Zhang, Y.; Zhao, G.; Coropceanu, V.; Hu, W.; Parkin, S.; Brédas, J.-L.; Briseno, A. L. Triisopropylsilyl-ethynyl-Functionalized Graphene-Like Fragment Semiconductors: Synthesis, Crystal Packing, and Density Functional Theory Calculations. *Chem. Eur. J.* **2013**, 19, 17907–17916.
- (22) Takimiya, K.; Bulgarevich, K.; Abbas, M.; Horiuchi, S.; Ogaki, T.; Kawabata, K.; Ablat, A. “Manipulation” of Crystal Structure by Methylthiolation Enabling Ultrahigh Mobility in a Pyrene-Based Molecular Semiconductor. *Adv. Mater.* **2021**, 33, 2102914.
- (23) Okamoto, T.; Yu, C. P.; Mitsui, C.; Yamagishi, M.; Ishii, H.; Takeya, J. Bent-Shaped *p*-Type Small-Molecule Organic Semiconductors: A Molecular Design Strategy for Next-Generation Practical Applications. *J. Am. Chem. Soc.* **2020**, 142, 9083–9096.
- (24) Jeong, E.; Ito, T.; Takahashi, K.; Koganezawa, T.; Hayashi, H.; Aratani, N.; Suzuki, M.; Yamada, H. Exploration of Alkyl Group Effects on the Molecular Packing of 5,15-Disubstituted Tetrabenzoporphyrins toward Efficient Charge-Carrier Transport. *ACS Appl. Mater. Interfaces* **2022**, 14, 32319–32329.
- (25) Baeg, K. J.; Binda, M.; Natali, D.; Caironi, M.; Noh, Y. Y. Organic Light Detectors: Photodiodes and Phototransistors. *Adv. Mater.* **2013**, 25, 4267–4295.
- (26) Takahashi, K.; Kuzuhara, D.; Aratani, N.; Yamada, H. Synthesis and Crystal Structures of 5,15-Bis(triisopropylsilyl-ethynyl)-tetrabenzoporphyrins. *J. Photopolym. Sci. Technol.* **2013**, 26, 213–216.
- (27) Takahashi, K.; Yamada, N.; Kumagai, D.; Kuzuhara, D.; Suzuki, M.; Yamaguchi, Y.; Aratani, N.; Nakayama, K.; Yamada, H. Effect of Alkyl Substituents: 5,15-Bis(trimethylsilyl-ethynyl)- vs. 5,15-Bis(triisopropylsilyl-ethynyl)-tetrabenzoporphyrins and their Metal Complexes. *J. Porphyrins Phthalocyanines* **2015**, 19, 465–478.
- (28) Zhu, J.; Hayashi, H.; Chen, M.; Xiao, C.; Matsuo, K.; Aratani, N.; Zhang, L.; Yamada, H. Single Crystal Field-Effect Transistor of Tetrabenzoporphyrin with a One-Dimensionally Extended Columnar Packing Motif Exhibiting Efficient Charge Transport Properties. *J. Mater. Chem. C* **2022**, 10, 2527–2531.
- (29) Sugano, Y.; Matsuo, K.; Hayashi, H.; Aratani, N.; Yamada, H. Synthesis and Properties of 10,20-Bis(triisopropylsilyl-ethynyl)-tetrabenz-5,15-diazaporphine. *J. Porphyrins Phthalocyanines* **2023**, 27, 136–144.
- (30) Takahashi, K.; Shan, B.; Xu, X.; Yang, S.; Koganezawa, T.; Kuzuhara, D.; Aratani, N.; Suzuki, M.; Miao, Q.; Yamada, H. Engineering Thin Films of a Tetrabenzoporphyrin toward Efficient Charge-Carrier Transport: Selective Formation of a Brickwork Motif. *ACS Appl. Mater. Interfaces* **2017**, 9, 8211–8218.
- (31) Tian, H.; Han, Y.; Bao, C.; Yan, D.; Geng, Y.; Wang, F. An Asymmetric Oligomer Based on Thienoacene for Solution Processed Crystal Organic Thin-Film Transistors. *Chem. Commun.* **2012**, 48, 3557–3559.
- (32) Inoue, S.; Minemawari, H.; Tsutsumi, J.; Chikamatsu, M.; Yamada, T.; Horiuchi, S.; Tanaka, M.; Kumai, R.; Yoneya, M.; Hasegawa, T. Crystal Structure of Asymmetric Organic Semiconductor 7-Decyl-2-phenyl[1]benzothieno[3,2-*b*][1]benzothiophene. *Chem. Mater.* **2015**, 27, 3809–3812.
- (33) Yamada, H.; Kushibe, K.; Mitsuogi, S.; Okujima, T.; Uno, H.; Ono, N. Selective Synthesis of 5-Alkenyl-15-alkynyl-porphyrin and 5,15-Dialkynyl-porphyrin by 2+2 Acid-Catalyzed Condensation of Dipyrromethane and TMS Propynal. *Tetrahedron Lett.* **2008**, 49, 4731–4733.
- (34) Tamura, Y.; Saeki, H.; Hashizume, J.; Okazaki, Y.; Kuzuhara, D.; Suzuki, M.; Aratani, N.; Yamada, H. Direct Comparison of a Covalently-Linked Dyad and a 1:1 Mixture of Tetrabenzoporphyrin and Fullerene as Organic Photovoltaic Materials. *Chem. Commun.* **2014**, 50, 10379–10381.
- (35) Jeong, E.; Takahashi, K.; Rajagopal, S. K.; Koganezawa, T.; Hayashi, H.; Aratani, N.; Suzuki, M.; Nguyen, T. Q.; Yamada, H. Orbital-Energy Modulation of Tetrabenzoporphyrin-Derived Non-Fullerene Acceptors for Improved Open-Circuit Voltage in Organic Solar Cells. *J. Org. Chem.* **2019**, 85, 168–178.
- (36) ADF2021, Scientific Computing & Modeling (SCM), Theoretical Chemistry, Vrije Universiteit, Amsterdam, The Netherlands, <http://www.scm.com>.